Aust. J. Phys., 1975, **28**, 85–99

Supersonic Neutral Winds in an Outer Atmosphere. III* A Two-dimensional Model

N. E. Gilbert

Division of Theoretical and Space Physics, La Trobe University; present address: Aeronautical Research Laboratories, P. O. Box 4331, Melbourne, Vic. 3001.

Abstract

A steady two-dimensional model that represents the part of a convection cell where the neutral gas constituent is rising and becoming supersonic is presented for both isothermal and variable temperature conditions in an intensely heated region of the outer atmosphere of a planet or star. The streamlines and orthogonal curves are represented by a system of confocal hyperbolae and ellipses respectively. The nozzle throat is achieved principally by the physical contraction and subsequent expansion of the gas rather than by a variation in the temperature or in the gravitational force component along the streamline. Regions in which supersonic speeds may be achieved are investigated by making suitable approximations both when the streamline is nearly vertical and when it approaches its asymptote. The characteristic patterns for the velocity and heating contours are shown, and the effects which parameters have in modifying these patterns are discussed.

Introduction

The conditions under which supersonic neutral winds may be achieved in the outer atmosphere of a planet have been explored for an isothermal environment in Part I of this series (Gilbert and Cole 1974*a*) and for the case of a variable temperature in Part II (Gilbert and Cole 1974*b*). In these studies, streamline functions suggested by the possible shapes of convection cells were chosen and the boundary walls of a narrow tube of gas about a streamline were defined in a convenient mathematical form. No attempt was made to match boundary walls of adjacent streamlines so that a fully two-dimensional model was not possible. For the same general assumptions, the present paper presents a steady two-dimensional model that represents the part of a convection cell where the gas is rising and becoming supersonic. Such a model is only appropriate in a region of intense heating, which may be caused, in the case of the Earth's atmosphere, by nuclear explosions or by auroral processes (Cole 1966), as was suggested in Part I.

The behaviour of the Earth's atmosphere in response to heating has been investigated previously for the more likely case of subsonic speeds. Thomas and Ching (1969) used analytical expressions in their study of the atmospheric response with altitude to various forms of time-dependent heating functions, while Volland and Mayr (1971) assumed small perturbations and known functional forms of the time-dependent variables to treat the time-dependent problem in three dimensions.

Under the assumption of incompressibility, convective motion has been studied in both a fluid mechanics and a meteorological context (Scorer and Ludlam 1953;

* Part II, *Aust. J. Phys.*, 1974, **27**, 529–40.

Batchelor 1954; Scorer 1957; Lilly 1964). The shape-preserving circulating vortex structure is generally referred to as a 'thermal'. Both experimental and theoretical evidence demonstrate that under certain conditions a thermal will rise and expand while retaining its shape. By considering a suitable space–time transformation (i.e. by stretching the coordinates), Lilly (1964) was able to obtain a pseudo steady-state solution asymptotically. Much work has been done on the motion of plumes and thermals (for a review, see Turner 1969) but, as in most meteorological studies, the gas is assumed to be incompressible; also, supersonic speeds are completely inappropriate. Assuming hydrostatic equilibrium for a planet's atmosphere, one may show that the density decreases exponentially with altitude (e.g. Nicolet 1960) so that, except for very small scale convection (where the cell size is of the order of magnitude of a few kilometres), the assumption of a constant density is unrealistic. More important in the present paper though is that to achieve a nozzle throat in the real, as opposed to ficticious, sense (see below) at which the flow becomes supersonic, the gas must contract and subsequently expand.

Generally, complete convection cells are modelled in which downward flow away from the centre is included. However, for convection in which the heating is so intense that supersonic speeds are achieved, only the rising gas may be suitably represented by a system of mathematically simple streamlines. Further away from the heating, even before the gas sinks, the motion would become turbulent. A closed system also presents problems in the steady-state case in that mechanisms for maintaining the energy balance must be invoked. A convenient model that adequately represents the rising part of a convection cell is that given by a system of confocal hyperbolae and ellipses (Lamb 1932). The streamlines are represented by the hyperbolae, while the orthogonal curves, necessary to determine the expansion or contraction rate of the gas, are represented by ellipses. This classical model is generally used to represent the flow of liquid from one side of a thin plane partition to the other through an aperture between the foci. In this way, a nozzle throat may be achieved principally by the physical contraction and subsequent expansion of the gas, rather than in the ficticious sense by variation in gravity itself (see Parker 1964, p. 91, for a mathematical demonstration of the equivalence), in the gravitational force component (Part I), in temperature (Part II), or in additional effects of friction (Banks and Holzer 1968). At the foci, the velocity is infinite (Lamb 1932), so that for the model to be physically meaningful, one of the hyperbolae must be regarded as an outer boundary wall each side of the centre.

Because the throat for each tube about a streamline is found to occur above the centre of the cell such that the streamline is nearly vertical, vertical supersonic wind components are achieved at the critical point, rather than the horizontal components envisaged in the earlier models of Parts I and II. Hence, more intense heating may be necessary for such a model to be physically possible. For the variation in velocity to be continuous along a curve orthogonal to the streamline (i.e. along an ellipse) between the outer boundary walls, a critical point must exist along each streamline. Therefore, it is not possible to have split regions such that for some of the streamlines, near the vertical for example, the velocity remains subsonic while for others the velocity becomes supersonic.

Regions in which supersonic speeds may be achieved are investigated here for both isothermal and variable temperature conditions. A convenient temperature profile is chosen such that a maximum occurs at the centre and the ellipses are themselves temperature contours. The conditions for achieving the following points are examined by making appropriate approximations:

(1) a 'single critical' point at which the velocity becomes supersonic,

(2) a 'stationary' point at which the velocity is a maximum, and

(3) an 'infinite acceleration' point at which the velocity decreases to the characteristic thermal velocity with negative infinite acceleration.

Finally, velocity and heating contours are presented to illustrate the characteristic behaviour and general effects of parameter variations.

Mathematical Model

In Parts I and II, streamline functions were chosen because they were suggested by the possible shapes of a part of a convection cell and for their mathematical convenience in simplifying the equations while allowing the existence of a critical point. The cross sectional area of a narrow expanding tube of gas was assumed to be proportional to the distance along the tube from its apex, raised to a power n. However, no attempt was made to form a composite model consisting of a number of tubes. For a two-dimensional model, streamlines must be chosen such that two adjacent streamlines have a common boundary wall. This condition is satisfied for the case of radial expansion in a vertical plane where $n = 1$. The upward diverging and upward converging parts of a convection cell could be separately represented by radial expansion and contraction respectively, but the main problem with such a model is in attempting to match both parts for a continuous flow from the lower part to the upper part. The simplest extension of this crude model that enables a perfect matching of both parts is to represent the streamlines by hyperbolae with a horizontal major axis and common foci and centre, the asymptotes being straight lines radiating from the centre (defined as the reference position and origin of the coordinate system). Orthogonal curves are given by ellipses having the same major axis, foci and centre as the hyperbolae (Lamb 1932). Radial flow is obtained away from the centre when the hyperbolae approach their respective asymptotes. Because the velocity is infinite at the foci, for the model to be physically meaningful one of the hyperbolae is assumed to form an outer boundary wall each side of the centre. On defining the angle between the asymptote of a hyperbola and the vertical as ϕ, such a boundary is arbitrarily chosen such that $\phi = 70°$.

It is convenient to write the variables in dimensionless form. For a reference length, the distance d from the cell centre to each focus is chosen and, provided d/a is negligible (where a is the distance from the planet centre to the reference position) and distances are not very much greater than d/a, a rectilinear coordinate system may be used rather than the more complicated curvilinear system of Parts I and II. Other reference parameters specified are the temperature at the origin θ_0 and the characteristic thermal speed at the origin c_0 ($= (R\theta_0)^{\frac{1}{2}}$, where R is the gas constant). As in Parts I and II, reference to supersonic speeds is interpreted to mean greater than the characteristic thermal speed c ($= (R\theta)^{\frac{1}{2}}$, where θ is the temperature), rather than the sonic speed $(\gamma R\theta)^{\frac{1}{2}}$, where γ is the ratio of the specific heats. Scaled by these reference parameters, the dimensionless variables are: x, the horizontal distance; y, the vertical distance; r, the distance along the streamline from the x axis (negative for $y < 0$); A, the arc length along an ellipse between boundary walls about a streamline; T, the temperature (θ/θ_0); and v, the velocity. Because of the symmetry about the y axis, the model is considered only for $x \geqslant 0$.

Given $x = x_0$ at $y = 0$, the streamlines are defined by

$$x^2/x_0^2 - y^2/a_x = 1\,, \tag{1}$$

where $a_x = 1 - x_0^2$, while, given $y = y_0$ at $x = 0$, the orthogonal curves are defined by

$$x^2/a_y + y^2/y_0^2 = 1\,, \tag{2}$$

where $a_y = 1 + y_0^2$. The distance along a streamline from the x axis is given by

$$r = \int_0^y \{(a_x^2 + y^2)/(a_x^2 + a_x y^2)\}^{\frac{1}{2}}\, \mathrm{d}y \tag{3}$$

and the arc length along an ellipse between x coordinates x_1 and x_2 ($x_2 > x_1$) is

$$A = \int_{x_1}^{x_2} \{(a_y^2 - x^2)/(a_y^2 - a_y x^2)\}^{\frac{1}{2}}\, \mathrm{d}x\,. \tag{4}$$

Both integrals in equations (3) and (4) cannot be evaluated analytically and hence they are calculated numerically using Simpson's rule. The angle Φ between the streamline and vertical is given by

$$\cos\Phi = \{(a_x^2 + a_x y^2)/(a_x^2 + y^2)\}^{\frac{1}{2}}\,. \tag{5}$$

Assuming only pressure gradient and gravitational forces for steady-state motion of a neutral gas constituent, the 'general nozzle flow equation' (Part I) may be written as (noting that the variables are now in dimensionless form and that the gravitational force is assumed constant)

$$(v - T/v)\mathrm{d}v/\mathrm{d}r = F(r)\,, \tag{6}$$

where

$$F(r) = F_1 + F_2 + F_3\,, \tag{7}$$

and

$$F_1 = A^{-1}\,\mathrm{d}A/\mathrm{d}r\,, \qquad F_2 = -T^{-1}\,\mathrm{d}T/\mathrm{d}r\,, \qquad F_3 = -\lambda T^{-1}\cos\Phi\,,$$

with $\lambda = g_0 d/R\theta_0$ and g_0 the gravitational acceleration at the reference position.

In dimensionless form, the net accession of heat Q from all sources and sinks may be written as (Part I)

$$Q = \frac{qd}{\rho_0 c_0^3} = \left(\frac{A_0 v_0}{Av}\right)\left(T\frac{\mathrm{d}v}{\mathrm{d}r} + \frac{v}{\gamma - 1}\frac{\mathrm{d}T}{\mathrm{d}r}\right), \tag{8}$$

where q is the net accession of heat in dimensional form and ρ_0 and v_0 are the density and velocity at the reference position.

A feasible temperature profile appropriate to an intensely heated region of an otherwise isothermal part of an atmosphere is one whereby a maximum occurs at the centre, the temperature decreases to a constant value away from the centre, and the ellipses are themselves the temperature contours; the last condition results in a constant maximum temperature along the x axis between the foci. A two-dimensional temperature profile may then be defined by a function along the y axis. The following Gaussian function for the temperature is therefore assumed:

$$T = T_\infty + (1 - T_\infty) \exp\{-(y_0/h)^2\}, \tag{9}$$

where T_∞ (<1) is the temperature approached asymptotically as $|y_0|$ tends to infinity, and h is the dimensionless temperature scale height. Given (x, y), the value of y_0 is first determined from equations (1) and (2) ($y_0 = y$ for $x = x_0 = 0$) so that T may be calculated from equation (9). However, $\mathrm{d}T/\mathrm{d}r$ must be calculated numerically.

Regions of Supersonic Speeds

It has been shown in Part I that, for a critical point to exist at which the velocity becomes supersonic, $F(r) = 0$ and $F'(r) > 0$, where the prime denotes differentiation with respect to r. With the present model, the gravitational force component does not in general vary significantly enough to achieve this condition without other effects being considered. Further away from the centre of the cell, where the flow becomes almost radial (see Part I), $F_1 \approx r^{-1}$, which approaches zero, as does F_2, as r becomes larger; F_3 approaches a constant negative value of $-(\lambda/T_\infty)\cos\phi$, so that $F(r)$ also approaches this value. Hence, provided $F(r)$ has one root such that $F'(r) > 0$, it will have another such that $F'(r) < 0$ and will asymptotically approach a constant negative value. This corresponds to the velocity becoming supersonic at the first zero, a maximum at the second zero, and ultimately to decrease to the characteristic thermal velocity with negative infinite acceleration. The model breaks down in this way because the assumptions of not too large distances are violated, and so the model must be restricted to regions within which the latter conditions may occur. For a velocity reversal to occur whereby the velocity decreases to a subsonic speed at a subsequent critical point, as described in Part II, $F(r)$ would have to possess another zero such that $F'(r) > 0$. Even if this were so, because $F(r)$ ultimately becomes negative the velocity would again become stationary, this time a minimum, and then increase to the characteristic thermal velocity with infinite acceleration. The following analysis examines the conditions for achieving a single critical point, stationary point and infinite acceleration point.

Critical Point

To achieve a critical point, $F(r)$ must increase on passing through a zero value. For the temperature profile defined by equation (9), the functions F_1 and F_2 are both negative when r is negative, zero when $r = 0$, positive when r is positive, and asymptotically approach zero as r tends to infinity. Since F_3 is always negative, $F(r)$ may only be positive for $r > 0$. For the isothermal case, where $F_2 = 0$, if the condition $F(r) > 0$ is to be satisfied, it must be so before the maximum value of F_1 is attained. This occurs well before the streamline approaches its asymptote, since in this region F_1 may be represented by the decreasing function r^{-1}. Because both r and A must be evaluated numerically from equations (3) and (4) respectively, the critical distance r_c or y_c (the subscript c denoting a critical value), which is found on solving the equation $F(r_c) = 0$, can only be determined numerically as in Parts I and II. To obtain an analytical solution for the isothermal case and to investigate the dependence of the critical distance on various parameters for both constant and variable temperature cases, F_1 may be approximated by (see Appendix) $F_1 = y/a_x^2$ provided $y^2 \ll a_x$, so that powers of y^2/a_x greater than unity may be neglected. By further

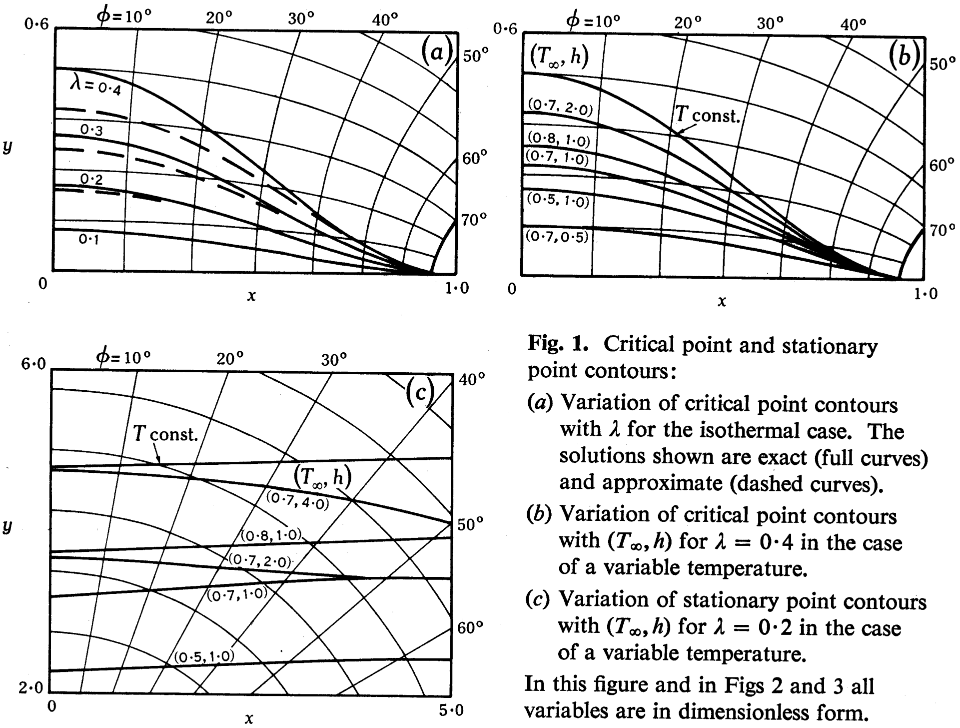

Fig. 1. Critical point and stationary point contours:

(*a*) Variation of critical point contours with λ for the isothermal case. The solutions shown are exact (full curves) and approximate (dashed curves).

(*b*) Variation of critical point contours with (T_∞, h) for $\lambda = 0 \cdot 4$ in the case of a variable temperature.

(*c*) Variation of stationary point contours with (T_∞, h) for $\lambda = 0 \cdot 2$ in the case of a variable temperature.

In this figure and in Figs 2 and 3 all variables are in dimensionless form.

neglecting y^2/a_x, F_3 may be approximated by $-\lambda/T$. Hence for the isothermal case, where $T = 1$,

$$y_c \approx \lambda a_x^2, \tag{10}$$

which at $x_0 = 0$ (that is, $a_x = 1$) results simply in $y_c \approx \lambda$. For consistency with the condition $y^2 \ll a_x$, the approximation (10) requires $\lambda^2 \ll a_x^{-3}$, and hence, noting that $a_x^{-3} \geqslant 1$, the condition $\lambda \leqslant 0 \cdot 4$ is imposed. At $x_0 = 0$, this latter condition requires $y \leqslant 0 \cdot 4$ for complete consistency.

For parameter λ, Fig. 1*a* shows the critical distance contours derived using the approximation in equation (10) compared with the exact values derived numerically. It may be observed that the contours all converge towards the focus, a result given directly by equation (10) when $x_0 = 1$ (that is, $a_x = 0$). At the focus, which is outside the outer boundary wall of the model considered, the velocity would be infinite. Physically, the closer the streamline is to the focus, the greater is the constriction of the flow below the horizontal axis of the convection cell, and the greater the subsequent expansion above the axis, so that a nozzle throat is achieved closer to the axis. With this model in the isothermal case, ignoring the slight variation in gravitational force component along a streamline (i.e. in $\cos\Phi$) for $y^2 \ll a_x$, a real nozzle throat is achieved rather than the ficticious or equivalent ones achieved earlier (Holzer and Axford 1970; Parts I and II).

Assuming that a critical point may be achieved in the isothermal case, the effect of the variable temperature, defined by equation (9), on the critical distance is required, given the same temperature-independent parameters. The validity of the above

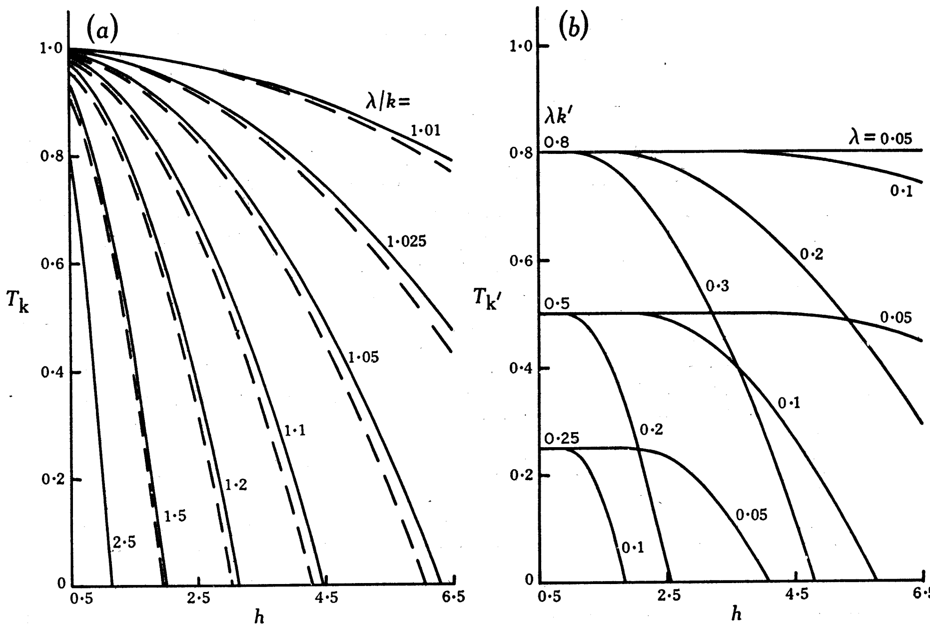

Fig. 2. Boundary values for T_∞, showing the variation with h of (a) T_k for parameter λ/k when $\lambda = 0\cdot05$ (full curves) and $0\cdot4$ (dashed curves), and (b) $T_{k'}$ for parameters $\lambda k'$ and λ.

approximations is always maintained if the additional effect does not increase y_c at $x = 0$. Assuming these approximations, at the critical point $(0, y_c)$ when the temperature is constant, the equation $F(r_c) = 0$ gives $y_c = r_c = \lambda$. When the temperature varies, the required condition $y_c \leqslant \lambda$ is equivalent to $F(\lambda) \geqslant 0$, which from equations (7) and (9) results in

$$\lambda^2 \leqslant h^2 \ln(1+2/h^2),$$

which does not depend on T_∞, noting though that $T_\infty < 1$. When λ is its maximum value of $0\cdot4$, h is approximately $\geqslant 0\cdot2$. Small values of h, much less than unity, though possible soon after heating commences when considering a time-dependent solution, are considered unrealistic under steady conditions, and hence the condition $h \geqslant 0\cdot5$ is imposed.

Fig. 1b shows how the critical point contours vary with the temperature profile parameters T_∞ and h for $\lambda = 0\cdot4$. The critical distance y_c is observed to decrease as both T_∞ and h decrease, that is, as the heating at the centre becomes more intense relative to the surrounding area.

As in Parts I and II, a general critical distance boundary value k corresponding to y_c (or r_c at $x_0 = 0$) is introduced such that $0 < k \leqslant 0{\cdot}4$. The value k represents the extreme upper boundary at $k = 0{\cdot}4$ and the 'limiting' extreme lower boundary as k approaches zero, but may be either a lower or upper boundary between. The condition $k \leqslant \lambda$ is necessary for consistency with the condition $y_c \leqslant \lambda$. On solving the equation $F(k) = 0$, an expression for the corresponding boundary value of T_∞, written as T_k, is given by

$$T_k = (B - \lambda k^{-1})/(B-1), \tag{11}$$

where

$$B = (1+2/h^2)\exp\{-(k/h)^2\}.$$

Table 1. Approximations for analysis of critical point

Expressions for F_1, F_2, F_3 and y_c are shown for three cases when $y^2 \ll a_x$ ($y \leqslant 0{\cdot}4$ at $a_x = 1$), $\lambda \leqslant 0{\cdot}4$ and $h \geqslant 0{\cdot}5$. The critical distance y_c is obtained by substituting y_c for y in the equation $F_1+F_2+F_3 = 0$ and can only be calculated numerically in case B

Function	Case A isothermal ($T = 1$)	Case B variable T $a_x = 1$	Case C variable T $a_x = 1$, $\lambda \ll 0{\cdot}5$, $y \leqslant \lambda \ll h$
F_1	y/a_x^2	y	y
F_2	0	$\{2y(T-T_\infty)/h^2\}T^{-1}$	$2y(1-T_\infty)/h^2$
F_3	$-\lambda$	λ/T	$-\lambda$
y_c	λa_x^2	—	$\lambda\{1+2(1-T_\infty)/h^2\}^{-1}$

For all h, B assumes its smallest value when k is its maximum value (i.e. $0{\cdot}4$). For $k = 0{\cdot}4$, B has a maximum value of about five at $h = 0{\cdot}417$. As h increases, B decreases, approaching unity asymptotically as h tends to infinity. Since we have $h \geqslant 0{\cdot}5$, it follows that B is greater than unity. Therefore, because $(B-1)$ must be positive in equation (11), a lower boundary at k, which is equivalent to the condition $F(k) < 0$, results in a lower boundary for T_∞. Similarly, an upper boundary at k results in an upper boundary for T_∞.

The variation of T_k with h for parameter λ/k when $\lambda = 0{\cdot}05$ and $0{\cdot}4$ is shown in Fig. 2*a*. Given a constant value of λ/k, for $\lambda \ll 0{\cdot}5$ (the minimum value of h), k must be very much less than h, since we have $k \leqslant \lambda$. Hence the exponential function in the expression for B above is approximately unity, so that T_k may be written as

$$T_k \approx 1 - \tfrac{1}{2}h^2(\lambda/k - 1), \tag{12}$$

which depends on λ/k rather than on λ and k separately. The curves in Fig. 2*a* when $\lambda = 0{\cdot}05$ (full curves) may be adequately represented by equation (12) and, even when λ is its largest value of $0{\cdot}4$ (dashed curves), the absolute error in T_k can be seen to be no more than about $0{\cdot}075$ within the range of h shown. Approximating $\exp\{-(k/h)^2\}$ in this way is equivalent to assuming that, in the interval for k, the temperature gradient is linear, that is,

$$\mathrm{d}T/\mathrm{d}y = -2y(1-T_\infty)/h^2,$$

and the temperature itself may be represented by a mean value ($T = 1$). The critical distance may then be written as

$$y_c \approx \lambda\{1+2(1-T_\infty)/h^2\}^{-1}.$$

The various approximations used for F_1, F_2 and F_3 when $y^2 \ll a_x$, and for the resulting expressions for y_c where appropriate, are summarized in Table 1.

Stationary Point

To achieve a stationary point r_s or y_s (the subscript s denoting a stationary value) following a critical point, $F(r)$ must decrease on passing through a subsequent zero value. F_1 may be represented by the decreasing function r^{-1} as the streamline approaches its asymptote (defined by $x = y\tan\phi$, where $\tan\phi = x_0 a_x^{-\frac{1}{2}}$). Thus, for the isothermal case, since F_3 is always negative $F(r)$ will ultimately become negative. As for r_c, without making approximations, r_s may only be determined numerically. Corresponding to the procedure adopted for examining the behaviour of the critical point, expressions are now derived for an approximation of y_s and a general boundary value for T_∞ at $x = 0$, and the validity of the approximations for the additional effect of the assumed temperature profile is investigated.

For $y^2 \gg a_x$, we have $F_1 \approx r^{-1}$ and $r \approx y\sec\phi$, the distance along the asymptote from the origin. Hence, for the isothermal case, the equation $F(r_s) = 0$ results in

$$y_s \approx \lambda^{-1}, \tag{13}$$

which, unlike the approximation for y_c, is independent of x_0. For consistency with the condition $y^2 \gg a_x$, the approximation (13) requires $\lambda^2 \ll a_x^{-1}$ and hence, noting that $a_x^{-1} \geqslant 1$, the same condition for λ (namely $\lambda \leqslant 0{\cdot}4$) is imposed as was when $y^2 \ll a_x$. At $x_0 = 0$, the condition $\lambda \leqslant 0{\cdot}4$ requires $y \geqslant 2{\cdot}5$ (that is, $y \geqslant 1/0{\cdot}4$) for complete consistency.

Assuming the above approximations, at the stationary point $(0, y_s)$ when the temperature is constant, the equation $F(r_s) = 0$ gives $y_s = r_s = \lambda^{-1}$. For the validity of the approximations to always be maintained, the additional variable temperature effect (for $h \geqslant 0{\cdot}5$) must not decrease y_s at $x = 0$, which is equivalent to the condition $F(\lambda^{-1}) \geqslant 0$ and results in

$$\lambda^{-2} \leqslant h^2 \ln(1+2/h^2).$$

The smallest value of the left-hand side of this inequality is $6{\cdot}25$ (when $\lambda = 0{\cdot}4$), but the maximum value of the right-hand side approaches two (when h tends to infinity). Hence, unlike the critical-distance case, it is not possible to specify conditions such that the validity of the approximations is always maintained. At $x = 0$, both y_c and y_s decrease as a result of the additional effect of the assumed temperature profile, so that while the approximation for the former improves, the approximation for the latter deteriorates.

Fig. 1*c* shows how the stationary point contours (calculated numerically) vary with T_∞ and h for $\lambda = 0{\cdot}2$. The constant-temperature contour is seen to approach its approximate value of $y_s = 5$ as x_0 becomes larger; this is to be expected because the condition $y^2 \gg a_x$ is more easily satisfied. As with y_c, y_s is observed to decrease as both T_∞ and h decrease.

A general stationary distance boundary value k' corresponding to y_s (or r_s at $x_0 = 0$) is introduced such that $k' = k^{-1}$ (k being defined in the previous subsection as the critical distance boundary value), and therefore $k' \geqslant 2\cdot5$. The corresponding value of T_∞, written as $T_{k'}$, is given by

$$T_{k'} = (\lambda k' - D)/(1-D), \tag{14}$$

where

$$D = (1+2/h^2)\exp\{-(k'/h)^2\}.$$

In the assumed ranges of k' and h (namely $k' \geqslant 2\cdot5$ and $h \geqslant 0\cdot5$) D is less than unity, so that a lower boundary at k', which is equivalent to the condition $F(k') > 0$, results in a lower boundary for T_∞. Similarly, an upper boundary at k' results in an upper boundary for T_∞.

Table 2. Approximations for analysis of stationary point

Expressions for F_1, F_2, F_3 and y_s are shown for three cases when $y^2 \gg a_x$ ($y \geqslant 2\cdot5$ at $a_x = 1$), $\lambda \leqslant 0\cdot4$ and $h \geqslant 0\cdot5$. The stationary distance y_s is obtained by substituting y_s for y in the equation $F_1+F_2+F_3 = 0$ and can only be calculated numerically in case B

Function	Case A isothermal ($T = 1$)	Case B variable T $a_x = 1$	Case C variable T $a_x = 1, y \gg h$
F_1	$\cos\phi/y$	$\cos\phi/y$	y^{-1}
F_2	0	$\{2y\sec\phi(T-T_\infty)/h^2\}T^{-1}$	0
F_3	$-\lambda\cos\phi$	$-\lambda\cos\phi/T$	$-\lambda/T_\infty$
y_s	λ^{-1}	—	T_∞/λ

Fig. 2*b* shows the variation of $T_{k'}$ with h for parameter $\lambda k'$ when $\lambda = 0\cdot05$, $0\cdot1$, $0\cdot2$ and $0\cdot3$. As with the critical-distance case, an approximation for $T_{k'}$ may be found: for $k' \gg h$ the exponential in the expression for D is approximately zero, so that $T_{k'}$ may be written as

$$T_{k'} \approx \lambda k', \tag{15}$$

which is equivalent to assuming that, in the interval for k', $T = T_\infty$ and $\mathrm{d}T/\mathrm{d}y = 0$. The stationary distance may then be written as

$$y_s \approx T_\infty/\lambda.$$

It may be observed in Fig. 2*b* that $T_{k'}$ approaches the constant value in equation (15) as h decreases and k' increases (k' increases as λ decreases since $\lambda k'$ is held constant).

The various approximations used in the analysis of the stationary point are summarized in Table 2.

Infinite Acceleration Point

Following a velocity reversal at a stationary point, both F_1 and F_2 approach zero as r becomes larger, while F_3 approaches a constant negative value. The acceleration will therefore ultimately become infinite (negatively) as v approaches c. Generally, the point at which this occurs, r_t or y_t (the subscript t denoting a value at the infinite acceleration point), can only be determined numerically by calculating the velocity from equation (6). However, for the constant-temperature case when $x_0 = 0$, the approximations made above may be used to give a relationship between y_t and λ.

When the temperature is constant, the velocity at both y_c and y_t is the same so that, for $r = y$ and $(y, v) = (y_t, c)$ in equation (11) of Part I,

$$\int_{y_c}^{y_t} F(y)\,\mathrm{d}y = 0, \tag{16}$$

a result similar to that obtained in equation (18) of Part II when considering solutions that pass through two critical points. At $x_0 = 0$, separate approximations were previously made for the regions $y^2 \ll 1$ and $y^2 \gg 1$. Since we have $y_t > y_s > 1 > y_c > 0$, an approximation is required for F_1 in the intermediate region, when y^2 is close to unity. The regions are therefore modified such that $0 < y \leqslant 1$ and $y > 1$ respectively (at $y = 1$, $F_1 = 1$ using both approximations). Noting that $y_c = \lambda$, equation (16) may be written as (see case A of Tables 1 and 2)

Table 3. Variation with λ of parameters for analysis of infinite acceleration point

See text for definitions of h_t and T_t

λ	y_t	h_t	T_t
0·4	5·9	0·65	0·58
0·3	9·2	0·61	0·68
0·2	16·7	0·55	0·82
0·1	42·6	0·49	1
0·05	102·7	0·44	1

$$\int_{\lambda}^{1} (y-\lambda)\,\mathrm{d}y + \int_{1}^{y_t} (y^{-1}-\lambda)\,\mathrm{d}y = 0, \tag{17}$$

which results in

$$\lambda y_t - \ln y_t = \tfrac{1}{2}(1+\lambda^2). \tag{18}$$

Given λ, y_t must be obtained numerically but, if y_t is known, λ may be easily derived. From Table 3, it is observed that y_t increases rapidly as λ decreases.

By also assuming the earlier approximations for T and $\mathrm{d}T/\mathrm{d}y$, so that we have $T = 1$ and $\mathrm{d}T/\mathrm{d}y = -2y(1-T_\infty)/h^2$ when $0 < y \leqslant 1$, and $T = T_\infty$ and $\mathrm{d}T/\mathrm{d}y = 0$ when $y > 1$, the additional effect of the assumed variable temperature on y_t may be examined. In place of equation (17), we have the equation (see case C of Tables 1 and 2)

$$\int_{\lambda}^{1} \{y-\lambda+2y(1-T_\infty)/h^2\}\,\mathrm{d}y + \int_{1}^{y_t} (y^{-1}-\lambda/T_\infty)\,\mathrm{d}y = 0,$$

which results in

$$\lambda y_t/T_\infty - \ln y_t = (1-T_\infty)\{(1-\lambda^2)/h^2 + \lambda/T_\infty\} + \tfrac{1}{2}(1+\lambda^2). \tag{19}$$

As with equation (18), y_t must be obtained numerically from (19). Since we have $y_t > y_s > 1$, it is not necessary for the additional effect to either increase or decrease y_t for the validity of the approximations to be maintained. However, to investigate the effect on y_t, assume arbitrarily that conditions for y_t to be decreased are required. Then, for y_t given by equation (18) we have

$$\int_{\lambda}^{y_t} F(y)\, dy < 0,$$

which results in

$$h^2 > (1-\lambda^2)T_\infty/\lambda(y_t-1).$$

Given λ, this inequality may be used to specify either a minimum value of h (written as h_t) or a maximum value of T_∞ (written as T_t) such that the additional effect of the variable temperature decreases the point y_t at which the acceleration becomes negatively infinite. The former is found when T_∞ approaches its maximum value of unity, while the latter is found when $h = 0 \cdot 5$, its minimum value. Consistent with the condition $T_\infty < 1$, we must have $T_t < 1$, and hence where the calculated value of T_t in Table 3 exceeds this limit it has been set equal to 1. It may be seen from Table 3 that, for $\lambda \leqslant 0 \cdot 1$, y_t will always be decreased by the additional effect for the assumed range of values for h and T_∞.

Velocity and Heating Solutions

Methods of solving the general nozzle flow equation (6) have been presented in Part I for the isothermal case and in Part II for the variable temperature case by using finite-difference formulae. Only the solutions themselves for the model under consideration are therefore presented here with appropriate comment. As discussed in Part I, comparisons with any experimental data are inappropriate at present.

Unlike the earlier models in Parts I and II, the present two-dimensional model achieves a nozzle throat in a more real sense in that the boundary walls about a streamline allow for contraction and subsequent expansion of the gas. At $x_0 = 0$ the gravitational force component is constant along the streamline, so that for a constant temperature, provided a critical point exists, there is a physically real deLaval nozzle. Because dimensionless coordinates have been used and the streamlines are rigidly defined within this system, the 'real nozzle' effect remains constant, so that a characteristic pattern for the velocity and heating contours might be expected. Hence the variations in the parameters λ, h and T_∞, noting the earlier restrictions (namely $\lambda \leqslant 0 \cdot 4$, $h \geqslant 0 \cdot 5$ and $T_\infty < 1$), would distort this pattern rather than completely change it.

A region of a convection cell is first chosen such that for the assumed value of λ ($0 \cdot 2$) the characteristic pattern of the contours is clear and the velocity is monotonically increasing for all possible values of h and T_∞ within their assumed ranges. Such a region is illustrated in Fig. 3, which shows the contours for v and Q when the temperature is constant compared with those when $h = 1$ and $T_\infty = 0 \cdot 7$. The observed effect in modifying the contours is found to be more pronounced as both h and T_∞ decrease, that is, as the heating at the centre becomes more intense relative to the surrounding area. For the isothermal case, Q will become negative following the stationary point (zero at the stationary point) while, for the variable temperature case, since $\mathrm{d}T/\mathrm{d}r < 0$ when $r > 0$, Q will become negative before the stationary point occurs. For a constant temperature, a decrease in λ shifts the velocity contours lower, but insignificantly affects the heating contours. Only Q depends on γ, and a decrease in γ has the same effect as a decrease in h or T_∞. From the characteristic pattern it may be concluded that closer to the focus the velocity increases more rapidly, and hence the heating is greatest there.

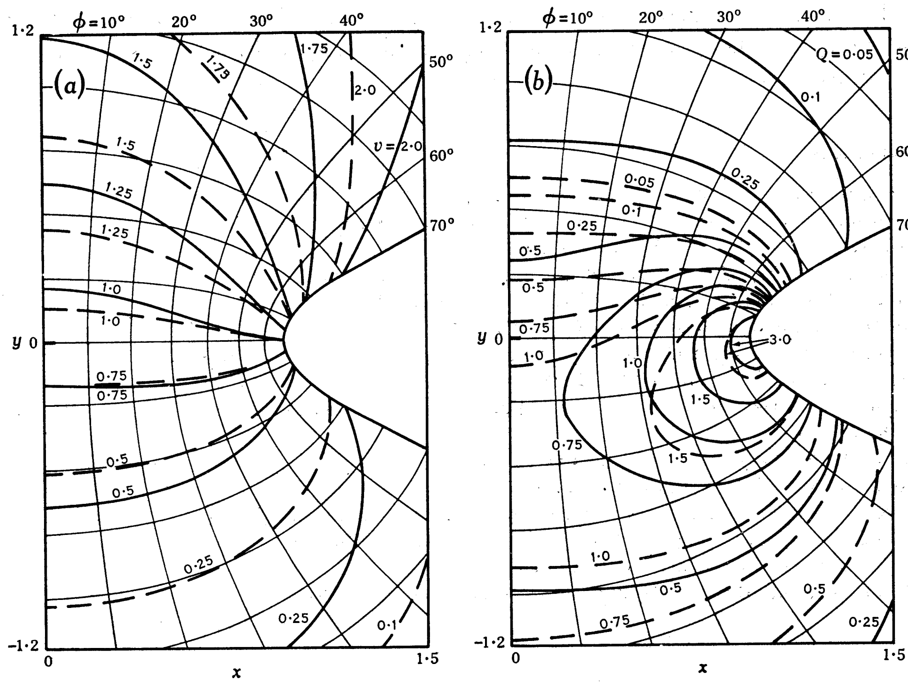

Fig. 3. Contours for (*a*) velocity v and (*b*) heating Q when $\lambda = 0\cdot 2$ for the isothermal case (full curves) and the variable temperature case when $T_\infty = 0\cdot 7$ and $h = 1$ (dashed curves). In (*b*) the specific heat ratio γ is taken to be $1\cdot 67$.

Conclusions

In the steady two-dimensional model considered here for the part of a convection cell where the neutral gas constituent is rising and becoming supersonic, under both isothermal and variable temperature conditions in an intensely heated region of the outer atmosphere of a planet or star, a classical system of confocal hyperbolae and ellipses has been used to represent the streamlines and orthogonal curves respectively. With this model, the nozzle throat has been found to be achieved principally by the physical contraction and subsequent expansion of the gas, rather than artificially by varying the temperature or the gravitational force component along the streamline. For the variation in velocity to be continuous along an ellipse between the outer boundary walls, it is not possible to have split regions such that, for some of the streamlines, the velocity remains subsonic while, for others, the velocity becomes supersonic. Suitable approximations have allowed an investigation of regions in which supersonic speeds may be achieved both when the streamline is nearly vertical and when it approaches its asymptote, and the points have been found at which the velocity becomes supersonic, is a maximum, and decreases to the characteristic thermal velocity with negative infinite acceleration. Parameter variations have been shown to only modify the characteristic pattern observed for the velocity and heating contours rather than completely alter it.

Acknowledgments

The author is indebted to the Aeronautical Research Laboratories, Melbourne, for the use of their excellent computing facilities and to Professor K. D. Cole for useful discussions.

References

Banks, P. M., and Holzer, T. E. (1968). *J. Geophys. Res.* **73**, 6846.
Batchelor, G. K. (1954). *Quart. J. Roy. Meteorol. Soc.* **80**, 339.
Cole, K. D. (1966). *Space Sci. Rev.* **5**, 699.
Gilbert, N. E., and Cole, K. D. (1974*a*). *Aust. J. Phys.* **27**, 511.
Gilbert, N. E., and Cole, K. D. (1974*b*). *Aust. J. Phys.* **27**, 529.
Holzer, T. E., and Axford, W. I. (1970). *Annu. Rev. Astron. Astrophys.* **8**, 31.
Lamb, H. (1932). 'Hydrodynamics', 6th Ed., p. 73 (Cambridge Univ. Press).
Lilly, D. K. (1964). *J. Atmos. Sci.* **21**, 83.
Nicolet, M. (1960). *In* 'Physics of the Upper Atmosphere' (Ed. J. A. Ratcliffe), p. 22 (Academic: New York).
Parker, E. N. (1964). *Astrophys. J.* **139**, 72.
Scorer, R. S. (1957). *J. Fluid Mech.* **2**, 583.
Scorer, R. S., and Ludlam, F. H. (1953). *Quart. J. Roy. Meteorol. Soc.* **79**, 94.
Thomas, G. E., and Ching, B. K. (1969). *J. Geophys. Res.* **74**, 1796.
Turner, J. S. (1969). *Annu. Rev. Fluid Mech.* **1**, 29.
Volland, H., and Mayr, H. G. (1971). *J. Geophys. Res.* **76**, 3764.

Appendix. Approximation for F_1 in the Region of a Critical Point

An approximation is required for F_1 $(= A^{-1}\,\mathrm{d}A/\mathrm{d}r)$ in the region of a critical point so that an analytical solution for the critical distance may be obtained when the temperature is constant. Noting that $x \geqslant 0$, equation (1) may be written as

$$x = x_0(1+y^2/a_x)^{\frac{1}{2}}.$$

Provided $y^2 \ll a_x$, so that powers of y^2/a_x greater than unity may be neglected, we have

$$x \approx x_0(1+y^2/2a_x), \qquad \mathrm{d}x/\mathrm{d}y \approx x_0\,y/a_x,$$

$$\cos\Phi \approx 1-\tfrac{1}{2}(x_0\,y/a_x)^2, \qquad r \approx y.$$

For a given streamline whose left boundary wall is defined by the hyperbola such that $x = x_0$ at $y = 0$, let the right boundary wall be defined by the hyperbola such that $x = x_0+A_0$ at $y = 0$, where A_0 is arbitrarily small. Then, further along the left wall at (x,y) the corresponding orthogonal point on the right wall may be approximated by $(x+A\sec\Phi, y)$, where A is the arc length approximated by the perpendicular distance between the point (x, y) and the hyperbola defining the right wall. Neglecting powers of A_0 greater than unity,

$$\{1-(x_0+A_0)^2\}^{-1} \approx a_x^{-1}(1+2A_0 x_0/a_x),$$

so that the right boundary wall may be approximated by the equation

$$x+A\sec\Phi \approx (x_0+A_0)(1+y^2/2a_x+y^2A_0 x_0/a_x^2).$$

Using the above approximations for x, $\cos\Phi$ and r,

$$(A/A_0)\sec\Phi \approx 1+y^2(1+x_0^2)/2a_x^2,$$

$$A/A_0 \approx 1+y^2/2a_x^2,$$

and F_1 is given by

$$F_1 = \frac{1}{A}\frac{\mathrm{d}A}{\mathrm{d}r} \approx \frac{A_0}{A}\frac{\mathrm{d}(A/A_0)}{\mathrm{d}y} \approx \frac{y}{a_x^2}.$$

Manuscript received 2 September 1974